Int. J. Solids Structures Vol. 16, pp. 131–148
Pergamon Press Ltd., 1980. Printed in Great Britain

AXISYMMETRIC AND BIFURCATION CREEP BUCKLING OF EXTERNALLY PRESSURISED SPHERICAL SHELLS

P. C. XIROUCHAKIS and NORMAN JONES†

Department of Ocean Engineering, Massachusetts Institute of Technology, Cambridge, MA 02139, U.S.A.

(Received 21 November 1978; in revised form 27 February 1979)

Abstract—The creep buckling behavior of a geometrically imperfect complete spherical shell subjected to a uniform external pressure is examined using Sanders' equilibrium and kinematic equations appropriately modified to include the influence of initial stress-free imperfections in the radius. The Norton–Bailey constitutive equations are used to describe the secondary creep behavior and elastic effects are retained. The initial imperfections have the same shape as the classical axisymmetric elastic buckling mode and the initial elastic response is obtained analytically for external pressures smaller than the corresponding static collapse pressure. Numerical finite-difference procedures are used to obtain the axisymmetrical creep buckling behavior and to determine when a bifurcation or loss of uniqueness into a non-axisymmetric deformation state occurs.

The numerical results for the creep buckling behavior of complete spherical shells are similar for hydrostatic and deadweight-type external pressures, at least for the particular parameters examined herein, and demonstrate that initial imperfections exercise an important influence on the critical times. It turns out from a practical viewpoint that axisymmetric creep buckling governs the behavior of the spherical shells examined in this article. It was observed from the present results that the creep buckling times of externally pressurised complete spherical shells are longer than those for "equivalent" axially loaded cylindrical shells.

NOTATION

- a mean radius of spherical shell
- c defined by eqn (16b)
- $e_{\alpha\beta}$ defined by eqn (9i)
- h thickness of spherical shell
- $k_{\alpha\beta}$ defined by eqn (9d)
- $m_{\alpha\beta}$, $n_{\alpha\beta}$ defined by eqns (9g, f)
- m circumferential harmonic (eqns 30)
- n degree of Legendre polynomial (eqn 15)
- p transverse pressure (Fig. 1)
- p_c $2Eh^2/\{3a^4(1-\nu^2)\}^{1/2}$, classical buckling pressure of an elastic perfect spherical shell
- p_s static buckling pressure of an elastic imperfect spherical shell
- q_α defined by eqn (9h)
- t time
- t_0 defined by eqn (8a)
- u_α, w non-dimensional displacements (eqns 9a, b)
- z coordinate normal to mid-surface of shell (Fig. 1)
- E Young's modulus
- $E_{\alpha\beta}$ membrane strains
- J_2 defined by eqn (3b)
- K creep coefficient (eqns 1, 2)
- K_M defined by eqn (2b)
- $K_{\alpha\beta}$ bending curvatures
- M defined by eqn (3a)
- $M_{\alpha\beta}$ bending moments per unit length (Fig. 1)
- N creep index (eqns 1–3)
- $N_{\alpha\beta}$ membrane forces per unit length (Fig. 1)
- P defined by eqn (8b)
- Q_α transverse shear forces per unit length (Fig. 1)
- T non-dimensional time (eqn 9l)
- T^c non-dimensional creep buckling time
- U_α, W in-plane and transverse displacements, respectively (Fig. 1)
- $\mathring{W}$ initial transverse displacement (imperfection)
- β circumferential coordinate (Fig. 1)
- ϵ radial imperfection non-dimensionalised with respect to h (eqn 15)
- $\epsilon_{\alpha\beta}$ defined by eqn (9c)
- ζ z/h
- $\eta_{\alpha\beta}$ total strain rate (eqn 4)
- $\eta_{\alpha\beta}^{EL}$ elastic strain (eqn 5)

†Present address: The University of Liverpool, Department of Mechanical Engineering, P.O. Box 147, Liverpool L69 3BX, England.

$\dot{\eta}^c_{\alpha\beta}$ creep strain rate (eqn 1)
θ meridional coordinate (Fig. 1)
λ_n defined by eqn (22d)
μ h/a
ν Poisson's ratio
$\sigma_{\alpha\beta}$ $\tau_{\alpha\beta}/E$
$\tau_{\alpha\beta}$ stress tensor for plane stress
ϕ_α rotations of middle surface
ϕ rotation of surface normal
ϕ_1 $= -\tilde{W}_{,1}/a$
ϕ_c defined by eqn (14a)
Φ_c defined by eqns (1) and (2)
$\mathcal{J}_2$ defined by eqn (14b)
$(\ )_{,1}$ $\partial(\ )/\partial\theta$
$(\ )_{,2}$ $\partial(\ )/\partial\beta$
$(\ )^*$ $\partial(\ )/\partial\theta$
$(\dot{\ })$ $\partial(\ )/\partial t$ or $\partial(\ )/\partial T$

INTRODUCTION

The creep buckling behavior of cylindrical shells subjected to various external loads has been examined by a number of authors as described in the review articles by Hoff[1] and Gerdeen and Sazawal[2]. Some more recent studies on the creep buckling of cylindrical shells are reported in Refs. [3–5]. By way of contrast, it is evident from Ref. [2] that relatively few investigations have been published on the creep buckling of spherical shells. The creep buckling behavior of spherical shells subjected to external pressures and made from materials prone to creep (e.g. plastics, concrete, titanium alloys) is of interest for the design of various ocean engineering structures (e.g. submersibles, habitats, underwater storage tanks).

The available theoretical studies on the creep buckling of viscoelastic spherical caps[6, 7, etc.], shallow spherical shells[8] and deep spherical shells[9, 10, etc.] were developed for shells with perfect geometries. However, it is well known[11, 12] that the static elastic and plastic buckling of spherical shells is sensitive to the influence of initial geometrical imperfections. A perturbation procedure was developed in Ref. [13] to examine the influence of an arbitrary initial imperfection field on the creep buckling behavior of a complete spherical shell subjected to a uniform external pressure. However, the theoretical results are only valid for small departures from the fundamental state and the influence of material elasticity was disregarded. Bushnell[14] has developed a numerical procedure which may be used for the creep buckling of shells but no results appear to have been published for spherical shells.

In this article, the creep buckling of an imperfect complete spherical shell subjected to a uniform external pressure is examined using Sanders'[15] equilibrium and kinematic equations appropriately modified to include the influence of initial stress-free imperfections in the radius. The Norton–Bailey constitutive equations are used to describe the secondary creep behavior and elastic effects are retained. The initial imperfections have the same shape as the classical axisymmetric elastic buckling mode[11, 16, 17, etc.] and the initial elastic response is obtained analytically for external pressures smaller than the corresponding static collapse pressure. Numerical finite-difference procedures are used to obtain the axisymmetrical creep buckling behavior and to determine when a bifurcation or loss of uniqueness into a non-axisymmetric deformation occurs.

The objective of this article is to reveal some aspects of the creep buckling behavior of externally pressurised imperfect complete spherical shells rather than to develop a numerical procedure which is suitable for a broader class of problems. The finite-difference energy scheme of Bushnell [14], which may be used for many structural problems, could have been employed for the present study. However, a different numerical procedure (finite-difference formulation of equilibrium equations) is used herein which embodies a few advantageous features for the present problem. For example, the initial elastic response is obtained analytically in the present work. Furthermore, all the èquations and results are dimensionless rather than dimensional as in Ref. [14]. The time integration scheme utilises a variable time step, which is more efficient particularly for creep problems, and Gauss–Legendre quadrature, which is more accurate than Simpson's rule, is used to evaluate the integrals across the shell thickness.

BASIC EQUATIONS

The strain-displacement and curvature change relations for the complete spherical shell in Fig. 1 are obtained in Ref. [18] according to Sander's non-linear shell equations for small strains and small rotations of the surface normal in comparison to rotations about the coordinate lines[15] and appropriately modified to include the effect of initial stress-free axisymmetric imperfections ($\bar{W}$). A consistent set of equilibrium equations were found using the principle of virtual work and reduce to the corresponding equations in Ref. [9] for the perfect case. The strain-displacement, curvature change, and equilibrium equations are given by eqns (1)–(13) in Ref. [18] and by eqns (10) and (11) here in dimensionless form.

Odqvist demonstrated that the Norton–Bailey law for uniaxial creep ($\dot{\eta}^c = K\tau^N$) when generalized with the aid of the Prandtl–Reuss incremental relations takes the form

$$\dot{\eta}^c_{\alpha\beta} = \Phi_c S_{\alpha\beta}, \tag{1}†$$

where $\dot{\eta}^c_{\alpha\beta}$ are the creep strain rates, $S_{\alpha\beta}$ is the stress deviator given by $S_{\alpha\beta} = \tau_{\alpha\beta} - \tau_{\gamma\gamma}\delta_{\alpha\beta}/3$,

$$\Phi_c = K_M J_2^M, \quad K_M = 3^{M+1}K/2, \tag{2a, b}$$

$$M = (N-1)/2, \quad \text{and} \quad J_2 = (\tau_{11}^2 + \tau_{22}^2 - \tau_{11}\tau_{22} + 3\tau_{12}^2)/3 \tag{3a, b}$$

for plane stress. The total strain rates are written as the sum of the elastic and creep components

$$\dot{\eta}_{\alpha\beta} = \dot{\eta}^{EL}_{\alpha\beta} + \dot{\eta}^c_{\alpha\beta}, \tag{4}$$

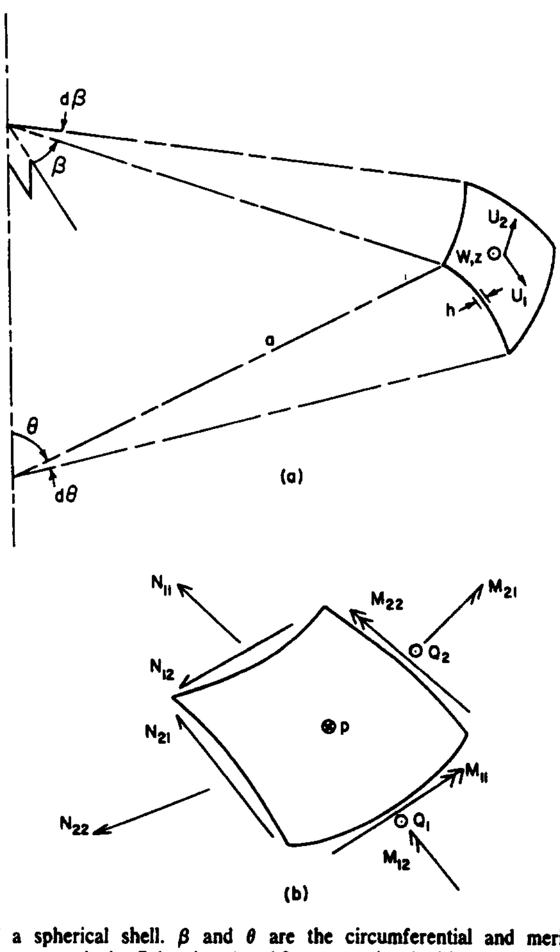

Fig. 1. Element of a spherical shell. β and θ are the circumferential and meridional coordinates, respectively. Subscripts 1 and 2 are associated with θ and β.

†Greek indices range from 1 to 2.

where the linear elastic strains are

$$\eta^{EL}_{\alpha\beta} = \{(1+\nu)\tau_{\alpha\beta} - \nu\tau_{\gamma\gamma}\delta_{\alpha\beta}\}/E \tag{5}$$

for an isotropic material. Equations (1), (4) and (5) give

$$\dot{\tau}_{12} = E\dot{\eta}_{12}/(1+\nu) - E\Phi_c\tau_{12}/(1+\nu) \tag{6a}$$

$$\dot{\tau}_{11} = E(\dot{\eta}_{11} + \nu\dot{\eta}_{22})/(1-\nu^2) - E\Phi_c\{(2-\nu)\tau_{11} - (1-2\nu)\tau_{22}\}/3(1-\nu^2), \tag{6b}$$

and a similar expression for $\dot{\tau}_{22}$.

Now the Love-Kirchoff assumption that initially plane cross sections remain plane throughout deformation requires $\dot{\eta}_{\alpha\beta} = \dot{E}_{\alpha\beta} + z\dot{K}_{\alpha\beta}$ so that defining the membrane forces ($N_{\alpha\beta}$) and bending moments ($M_{\alpha\beta}$) in the usual manner and using eqns (6) gives

$$\dot{N}_{11} = hE(\dot{E}_{11} + \nu\dot{E}_{22})/(1-\nu^2) - E\int_{-h/2}^{h/2}\Phi_c\{(2-\nu)\tau_{11} - (1-2\nu)\tau_{22}\}\,\mathrm{d}z/3(1-\nu^2), \tag{7}$$

together with expressions for the remainder of $\dot{N}_{\alpha\beta}$ and $\dot{M}_{\alpha\beta}$ which are presented in Ref. [18].

NON-DIMENSIONALISATION

The time t_0 required to reach a uniaxial strain η^c is $t_0 = \eta^c/K\tau^N$ according to eqn (1) for a time-independent uniaxial stress τ. If the uniaxial stress τ is identified with the membrane stress in a spherical shell due to a pressure p, then $\tau = pa/2h$. Thus, the time t_0 required for the creep strain η^c to reach the elastic strain given by $\eta^{EL} = \tau/E$ is $t_0 = 1/(KE\tau^{N-1})$, or

$$t_0 = (2/P)^{N-1}/KE^N, \quad P = pa/Eh. \tag{8a, b}$$

The dimensionless quantities

$$\begin{aligned} &u_\alpha = U_\alpha/h,\ w = W/h,\ \epsilon_{\alpha\beta} = a\eta_{\alpha\beta}/h,\ k_{\alpha\beta} = aK_{\alpha\beta},\\ &\mu = h/a,\ n_{\alpha\beta} = N_{\alpha\beta}/Eh,\ m_{\alpha\beta} = M_{\alpha\beta}/Eh^2,\ q_\alpha = Q_\alpha/Eh,\\ &e_{\alpha\beta} = aE_{\alpha\beta}/h,\ \sigma_{\alpha\beta} = \tau_{\alpha\beta}/E,\ \zeta = z/h, \text{ and } T = t/t_0, \end{aligned} \tag{9a–l}$$

together with eqn (8b) allow eqns (1)–(13) in Ref. [18] and eqns (4), (5) and (7) here to be written

$$\begin{aligned} &\phi_1 = \mu(u_1 - w_{,1}),\ \phi_2 = \mu(u_2 - w_{,2}\operatorname{cosec}\theta),\ \bar{\phi}_1 = -\mu\bar{w}_{,1},\\ &\phi = \mu(u_2\cot\theta + u_{2,1} - u_{1,2}\operatorname{cosec}\theta)/2,\\ &e_{11} = w + u_{1,1} + (\phi_1^2 + \phi^2)/2\mu + \phi_1\bar{\phi}_1/\mu,\\ &e_{22} = w + u_1\cot\theta + u_{2,2}\operatorname{cosec}\theta + (\phi_2^2 + \phi^2)/2\mu,\\ &e_{12} = \{u_{2,1} + u_{1,2}\operatorname{cosec}\theta - u_2\cot\theta + (\phi_1 + \bar{\phi}_1)\phi_2/\mu\}/2,\\ &k_{11} = \phi_{1,1},\ k_{22} = \phi_{2,2}\operatorname{cosec}\theta + \phi_1\cot\theta,\\ &k_{12} = (\phi_{2,1} + \phi_{1,2}\operatorname{cosec}\theta - \phi_2\cot\theta)/2, \end{aligned} \tag{10a–j}$$

$$\begin{aligned} &n_{11,1} + n_{11}\cot\theta + n_{12,2}\operatorname{cosec}\theta - n_{22}\cot\theta + q_1 - (\phi_1 + \bar{\phi}_1)n_{11}\\ &\qquad - \phi_2 n_{12} - \{\phi(n_{11} + n_{22})\}_{,2}\operatorname{cosec}\theta/2 - P(\phi_1 + \bar{\phi}_1) = 0,\\ &n_{22,2} + 2n_{12}\cos\theta + n_{12,1}\sin\theta + q_2\sin\theta - \{\phi_2 n_{22} + (\phi_1 + \bar{\phi}_1)n_{12}\}\sin\theta\\ &\qquad + \{\phi(n_{11} + n_{22})\}_{,1}\sin\theta/2 - P\phi_2\sin\theta = 0,\\ &q_{1,1} + q_1\cot\theta + q_{2,2}\operatorname{cosec}\theta - n_{11} - n_{22} - \{(\phi_1 + \bar{\phi}_1)n_{11} + \phi_2 n_{12}\}_{,1}\\ &\qquad - \{(\phi_1 + \bar{\phi}_1)n_{11} + \phi_2 n_{12}\}\cot\theta - \{(\phi_1 + \bar{\phi}_1)n_{12} + \phi_2 n_{22}\}_{,2}\operatorname{cosec}\theta - P = 0, \end{aligned}$$

$$m_{11,1}+m_{11}\cot\theta+m_{12,2}\operatorname{cosec}\theta-m_{22}\cot\theta-q_1/\mu=0,$$

$$m_{22,2}+2m_{12}\cos\theta+m_{12,1}\sin\theta-q_2\sin\theta/\mu=0, \tag{11a–e}$$

$$\dot{\epsilon}^{c}_{\alpha\beta}=\dot{\epsilon}_{\alpha\beta}-\dot{\epsilon}^{EL}_{\alpha\beta},\ \dot{\epsilon}^{EL}_{\alpha\beta}=\{(1+\nu)\dot{\sigma}_{\alpha\beta}-\nu\dot{\sigma}_{\gamma\gamma}\delta_{\alpha\beta}\}/\mu,$$

$$\dot{\epsilon}_{\alpha\beta}=\dot{e}_{\alpha\beta}+\zeta\dot{k}_{\alpha\beta}, \tag{12a–c}$$

$$\dot{n}_{11}=\mu(\dot{e}_{11}+\nu\dot{e}_{22})/(1-\nu^2)-\int_{-1/2}^{1/2}\phi_c\{(2-\nu)\sigma_{11}-(1-2\nu)\sigma_{22}\}\,d\zeta/3(1-\nu^2), \tag{13}$$

where

$$\phi_c=3^{(N+1)/2}(2/P)^{N-1}\mathcal{J}_2^{(N-1)/2}/2 \tag{14a}$$

$$\mathcal{J}_2=(\sigma_{11}^2+\sigma_{22}^2-\sigma_{11}\sigma_{22}+3\sigma_{12}^2)/3, \tag{14b}$$

and

$$(\dot{\ })=\partial(\ )/\partial T. \tag{14c}$$

Equations (10a–d), (10e–g) and (10h–j) are the dimensionless rotations, membrane strains and curvature changes, respectively, while eqns (11a–c) and (11d, e) are the respective three dimensionless force equilibrium equations and two moment equilibrium equations[15, 18].

INITIAL ELASTIC RESPONSE

A uniformly distributed external pressure is applied "instantaneously" but quasi-statically to the entire external surface area of a complete spherical shell. Thus, the initial condition for the creep buckling problem is the initial elastic response which is sought in this section. Only external pressures smaller than the corresponding elastic buckling pressure are of interest in this article.

The initial stress-free axisymmetric radial imperfection is assumed to have the form

$$\tilde{w}=\epsilon P_n(\cos\theta) \tag{15}$$

which is the shape of the elastic bifurcation mode† [11, 16, 17, etc], where $\tilde{w}$ is the non-dimensional radial displacement due to the presence of the non-dimensional radial imperfection of magnitude ϵ ($\tilde{w}$ and ϵ are non-dimensionalised with respect to the shell thickness), and P_n $(\cos\theta)$ is a Legendre polynomial of degree n. The value of n is the integer which most closely satisfies

$$n(n+1)=2ca/h,\ c=\sqrt{[3(1-\nu^2)]}. \tag{16a, b‡}$$

Now,

$$\phi_2=\phi=e_{12}=k_{12}=n_{12}=m_{12}=q_2=\tau_{12}=0$$

for the axisymmetrical behavior of a spherical shell and all the remaining variables are independent of β. A solution of the governing equations is sought to first order in ϵ using a perturbation scheme around the membrane state of deformation with

$$w=\bar{w}+\epsilon w',\ \text{and}\ u=\epsilon u', \tag{17a, b}$$

where $\bar{w}$ is the radial displacement according to the membrane solution and $\epsilon w'$ and $\epsilon u'$ are perturbations of order ϵ from the dominant membrane state. The zero order problem is the

†The perturbation procedure developed in Ref. [13] demonstrated that the critical harmonic for the creep buckling of a complete spherical shell was the same as the corresponding value for an elastic shell reported in Ref. [11, 16] and [17] with $\nu=0.5$.

‡It may be shown that the governing equations in this article also predict eqn (16a) and $p_c=2Eh^2/\{3a^4(1-\nu^2)\}^{1/2}$.

classical membrane solution[18]

$$\bar{w} = -(1-\nu)P/2\mu, \tag{18}$$

while the first order problem may be cast into the following form[18]

$$\begin{aligned}(1+\nu)w'^{*} + \nabla^2 s^{*} - (\nu + \cot^2\theta)s^{*} + \mu(1+\nu)\bar{w}\bar{w}^{*} + \mu^2\{\nabla^2 s^{*} - (\nu+\cot^2\theta)s^{*} \\ - \nabla^2 w'^{*} + (\nu + \cot^2\theta)w'^{*}\}/12 - \mu(1+\nu)\bar{w}(s^{*} - w'^{*}) \\ + 2\mu(1+\nu)\bar{w}(s^{*} - w^{*} - \bar{w}^{*}) = 0,\end{aligned} \tag{19a}$$

and

$$\mu(\nabla^2 + 1 - \nu)\nabla^2(s - w')/\{12(1+\nu)\} - (2w' + \nabla^2 s)/\mu + \bar{w}\nabla^2(w' + \bar{w} - s) = 0, \tag{19b}$$

where

$$s^{*} = u', \quad \text{and} \quad \nabla^2(\ ) = (\ )^{**} + \cot\theta(\ )^{*}. \tag{20a, b}$$

If

$$w' = A_n P_n(\cos\theta), \quad \text{and} \quad u' = B_n P_n{}^{*}(\cos\theta) \tag{21a, b}$$

are substituted into eqns (19) then it may be shown that the two resulting equations for A_n and B_n have the solution

$$A_n = \mu\bar{w}\{n(n+1) + 2\nu - \mu^2\lambda_n/6\}/\text{Det.}, \tag{22a}$$

$$B_n = \mu\bar{w}[1 + \nu + 2(1+\nu)/\{n(n+1)\} - \mu^2\lambda_n/6]/\text{Det.}, \tag{22b}$$

where

$$\begin{aligned}\text{Det.} = \{(1+\nu)(1-\mu\bar{w}) - \mu^2\lambda_n/12\}[1 + \mu\bar{w} - \mu^2\lambda_n/\{12(1+\nu)\}] \\ - \{(1+\mu^2/12)\lambda_n + (1+\nu)\mu\bar{w}\}[\mu^2\lambda_n/\{12(1+\nu)\} - 2/\{n(n+1)\} - \mu\bar{w}],\end{aligned} \tag{22c}$$

and

$$\lambda_n = 1 - \nu - n(n+1). \tag{22d}$$

Thus,

$$w = \bar{w} + \epsilon A_n P_n(\cos\theta), \quad \text{and} \quad u = \epsilon B_n P_n^{*}(\cos\theta) \tag{23a, b}$$

are the required solutions.

It may be shown[18] by taking the appropriate limits as θ approaches 0 or π that

$$u = \phi = q = 0, \; w = \bar{w} \pm \epsilon A_n, \tag{24a–d}$$

$$\begin{aligned}e_{11} &= \bar{w} \pm \epsilon\{A_n - n(n+1)B_n/2\}, \; e_{22} = e_{11}, \\ k_{11} &= \mp \epsilon\mu(B_n - A_n)n(n+1)/2, \; k_{22} = k_{11}, \\ n_{11} &= \mu\bar{w}/(1-\nu) \pm \epsilon\mu n(n+1)B_n/2(1+\nu), \; n_{22} = n_{11}, \\ m_{11} &= \pm\epsilon\mu^2(B_n - A_n)n(n+1)/\{24(1-\nu)\}, \; m_{22} = m_{11},\end{aligned} \tag{25a–h}$$

where the upper signs of $\pm$ or $\mp$ are used at $\theta = 0$ when n is even or odd and at $\theta = \pi$ for n even, while the lower sign is used at $\theta = \pi$ when n is odd.

AXISYMMETRIC CREEP BUCKLING

The governing equations for the creep buckling behavior of a complete spherical shell subjected to a uniform external pressure are developed in Ref. [18] using eqns (10)–(12) here for the case when the deformations remain axisymmetric. It turns out that these equations may be reduced to six first order differential equations in six rate variables $\dot{n}_{11}$, $\dot{q}$, $\dot{m}_{11}$, $\dot{u}$, $\dot{w}$ and $\dot{\phi}$ and written in the form

$$\dot{\bar{Z}}^* + \bar{A}\dot{\bar{Z}} = \bar{P}, \tag{26}$$

where

$$\dot{\bar{Z}} = [\dot{n}_{11}, \dot{q}, \dot{m}_{11}, \dot{u}, \dot{w}, \dot{\phi}]^T, (\ )^* = \partial(\ )/\partial\theta, \tag{27}$$

and the elements of the 6×6 matrix $\bar{A}$ and the 6×1 vector $\bar{P}$ are given in Appendix 1. It is evident from Appendix 1 that the elements of matrix $\bar{A}$ depend on the vector $\bar{Z}$, while vector $\bar{P}$ depends on the current state of stress $(\sigma_{11},\sigma_{22})$. Obrecht[5] successfully employed a similar formulation and choice of variables in a numerical analysis of the axial creep buckling of circular cylindrical shells. It appears that the present method has not been used to investigate the creep buckling behavior of imperfect complete spherical shells subjected to a uniform external pressure. A similar procedure was used previously with success to examine the plastic behavior of complete spherical shells[11] and to study the elastic behavior of shells of revolution in Refs.[19–21]. The advantage of this formulation is that no differentiation of the stiffness quantities is required as noted in Refs. [5 and 11].

The boundary conditions at the poles ($\theta = 0, \pi$) are

$$\dot{q} = \dot{u} = \dot{\phi} = 0. \tag{28}$$

BIFURCATION

The conditions under which a complete spherical shell which is deforming in the fundamental axisymmetric mode considered in the last section bifurcates into an asymmetric shape at some time T^b after creep commences are explored in this section. The constitutive equations for the incremental deformations from the fundamental axisymmetric state at the bifurcation time T^b are assumed to be elastic since the bifurcation occurs instantaneously[5, 22, etc.].

Let,

$$\begin{gathered}
u_1 = \bar{u}_1 + u_1', u_2 = u_2', w = \bar{w} + w', \phi_1 = \bar{\phi}_1 + \phi_1',\\
\phi_2 = \phi_2', \phi = \phi', e_{11} = \bar{e}_{11} + e_{11}', e_{22} = \bar{e}_{22} + e_{22}',\\
e_{12} = e_{12}', k_{11} = \bar{k}_{11} + k_{11}', k_{22} = \bar{k}_{22} + k_{22}', k_{12} = k_{12}',\\
n_{11} = \bar{n}_{11} + n_{11}', n_{22} = \bar{n}_{22} + n_{22}', n_{12} = n_{12}', q_1 = \bar{q}_1 + q_1',\\
q_2 = q_2', m_{11} = \bar{m}_{11} + m_{11}', m_{22} = \bar{m}_{22} + m_{22}', m_{12} = m_{12}',
\end{gathered} \tag{29a–t}$$

where the barred quantities now correspond to the axisymmetric state considered in the previous section, which includes both elastic and creep response, while the primed terms are the linear elastic perturbations from the fundamental axisymmetric state.

The strain-displacement, curvature change and equilibrium equations for the perturbed state are obtained by substituting eqns (29) into eqns (10) and (11) [18]. As remarked previously, the constitutive relations for the incremental perturbations from the axisymmetric state are governed by the linear elastic relationships. The β dependence may be eliminated from these equations by using[9]

$$u_1'(\theta,\beta) = u_1''(\theta)\sin m\beta, \text{ and } u_2'(\theta,\beta) = u_2''(\theta)\cos m\beta \tag{30a, b}$$

together with

$$(w', \phi_1', e_{11}', e_{22}', k_{11}', k_{22}', n_{11}', n_{22}', q_1', m_{11}', m_{22}') = (w'', \phi_1'', e_{11}'', e_{22}'', k_{11}'', k_{22}'', n_{11}'', n_{22}'', q_1'', m_{11}'', m_{22}'') \sin m\beta, \tag{30c}$$

and

$$(\phi', \phi_2', e_{12}', k_{12}', n_{12}', q_2', m_{12}') = (\phi'', \phi_2'', e_{12}'', k_{12}'', n_{12}'', q_2'', m_{12}'') \cos m\beta. \tag{30d}$$

It is shown in Ref. [18] that the governing equations for the asymmetrical bifurcation of a complete spherical shell may be reduced to the system of four second order differential equations

$$\bar{E}\bar{X}^{**} + \bar{F}\bar{X}^{*} + \bar{G}\bar{X} = 0, \tag{31a}$$

where the double primes are dropped for convenience,

$$(\ )^* = \partial(\ )/\partial\theta,$$
$$\bar{X} = [u_1, u_2, w, m_{11}]^T, \tag{31b}$$

and the elements of the 4×4 matrices $\bar{E}$, $\bar{F}$ and $\bar{G}$ are given in Appendix 2.

NUMERICAL PROCEDURE

(a) *Axisymmetric creep buckling*

The system of eqns (26) is solved using the central finite-difference method with a meridian of the shell ($0 \le \theta \le \pi$) divided into $N-1$ equally spaced intervals with N stations. Thus, eqn (26) becomes

$$(\hat{Z}^*)_{i-1/2} + (\bar{A}\hat{Z})_{i-1/2} = (\bar{P})_{i-1/2}, \tag{32}$$

where

$$\bar{Z}_{i-1/2} = (\bar{Z}_i + \bar{Z}_{i-1})/2$$

and

$$\bar{Z}^*_{i-1/2} = (\bar{Z}_i - \bar{Z}_{i-1})/\Delta\theta. \tag{33a, b}$$

If the finite-difference approximations (33) are substituted into eqn (32) then

$$\bar{F}_{i-1/2}\hat{Z}_{i-1} + \bar{G}_{i-1/2}\hat{Z}_i = \bar{P}_{i-1/2}, i = 2, 3, \ldots N, \tag{34}$$

where

$$\bar{F}_{i-1/2} = (\bar{A}_{i-1/2})/2 - \bar{I}/\Delta\theta, \bar{G}_{i-1/2} = (\bar{A}_{i-1/2})/2 + \bar{I}/\Delta\theta \tag{35a, b}$$

and $\bar{I}$ is the identity matrix. The elements of the 6×6 matrix $\bar{A}_{i-1/2}$ and the 6×1 vector $\bar{P}_{i-1/2}$ are given in Appendix 1.

Equations (34) may be recast in the form

$$\bar{F}^1_{2i-2}\hat{X}_{i-1} + \bar{F}^2_{2i-2}\hat{Y}_{i-1} + \bar{G}^1_{2i-2}\hat{X}_i + \bar{G}^2_{2i-2}\hat{Y}_i = \bar{P}^1_{2i-2}, \tag{36a}$$

and

$$\bar{F}^3_{2i-1}\hat{X}_{i-1} + \bar{F}^4_{2i-1}\hat{Y}_{i-1} + \bar{G}^3_{2i-1}\hat{X}_i + \bar{G}^4_{2i-1}\hat{Y}_i = \bar{P}^2_{2i-1} \tag{36b}$$

when the vector $\hat{Z}_i$ is split into the two subvectors $\hat{X}_i$ and $\hat{Y}_i$, where $\hat{X}_i = [\dot{n}_{11}, \dot{q}, \dot{m}_{11}]_i^T$, $\hat{Y}_i = [\dot{u}, \dot{w}, \dot{\phi}]_i^T$,

$$\bar{F}_{i-1/2} = \begin{bmatrix} \bar{F}^1_{2i-2} & \bar{F}^2_{2i-2} \\ \bar{F}^3_{2i-1} & \bar{F}^4_{2i-1} \end{bmatrix}_{i-1/2},$$

$$\bar{G}_{i-1/2} = \begin{bmatrix} \bar{G}^1_{2i-2} & \bar{G}^2_{2i-2} \\ \bar{G}^3_{2i-1} & \bar{G}^4_{2i-1} \end{bmatrix}_{i-1/2}, \quad \bar{P}_{i-1/2} = \begin{bmatrix} \bar{P}^1_{2i-2} \\ \bar{P}^2_{2i-1} \end{bmatrix}_{i-1/2}. \tag{37a–e}$$

Now, the boundary conditions at $\theta = 0$ and $\theta = \pi$ are given by eqns (28). The boundary conditions at $\theta = 0$ may be written in the form of eqn (36b) with $i = 1$ provided

$$\bar{F}_1^3 = \bar{F}_1^4 = \bar{P}_1^2 = 0, \tag{38a–c}$$

$$\bar{G}_1^3 = \begin{pmatrix} 0 & 0 & 0 \\ 0 & 1 & 0 \\ 0 & 0 & 0 \end{pmatrix}, \text{and } \bar{G}_1^4 = \begin{pmatrix} 1 & 0 & 0 \\ 0 & 0 & 0 \\ 0 & 0 & 1 \end{pmatrix}. \tag{38d, e}$$

Similarly, the boundary conditions at $\theta = \pi$ are given by eqn (36a) with $i = N + 1$ when

$$\bar{G}^1_{2N} = \bar{G}^2_{2N} = \bar{P}^1_{2N} = 0, \tag{39a–c}$$

$$\bar{F}^1_{2N} = \begin{pmatrix} 0 & 0 & 0 \\ 0 & 1 & 0 \\ 0 & 0 & 0 \end{pmatrix}, \text{and } \bar{F}^2_{2N} = \begin{pmatrix} 1 & 0 & 0 \\ 0 & 0 & 0 \\ 0 & 0 & 1 \end{pmatrix}. \tag{39d, e}$$

Thus, eqns (28) may be written

$$\bar{G}_1^3\hat{X}_1 + \bar{G}_1^4\hat{Y}_1 = 0, \text{and } \bar{F}^1_{2N}\hat{X}_N + \bar{F}^2_{2N}\hat{Y}_N = 0. \tag{40a, b}$$

The system of linear algebraic eqns (36) and (40) in the variables $\hat{X}_i$ and $\hat{Y}_i$ are solved at each time step using Potters' method [23, 24] and the initial conditions are given by the initial elastic response. The integration through the thickness of the shell required for the evaluation of $\bar{P}_{i-1/2}$ given by eqn (37e) and in Appendix 1 is done using the ten-point formula of Gauss–Legendre quadrature [25] which is more accurate than equal-interval formulae (e.g. Simpson's rule) for the same number of integration points.

The time integration of $\hat{Z}$ is performed by using Euler's integration scheme. It may be shown that eqn (53) in Ref. [26] can be written

$$\Delta T \le 4(1+\nu)[2\sqrt{(3\mathcal{J}_2)}/P]^{1-N}/3N \tag{41†}$$

and provides an upper bound on the time step ΔT to ensure numerical stability of the time integration scheme. If at each time step $\mathcal{J}_2$ is evaluated at every spatial point and the value of $\mathcal{J}_2$ in eqn (41) is identified with the maximum value of $\mathcal{J}_2(\mathcal{J}_{2(\max)})$, then the required time step is

$$\Delta T = 4f(1+\nu)\{2\sqrt{(3\mathcal{J}_{2(\max)})}/P\}^{1-N}/3N, \tag{42†}$$

where f is a factor less than unity. A result similar to eqn (42) was derived in Ref. [27] by requiring the incremental equivalent creep strain at each time step to be smaller than the corresponding equivalent elastic strain. It turns out in this case that the factor $4f(1+\nu)/3N$† in eqn (42) must be smaller than unity.

(b) *Bifurcation*

The system of eqns (31a) is solved using the central finite-difference method with a meridian of the shell $(0 \le \theta \le \pi)$ divided into N equally spaced intervals with $N + 1$ stations.

†N is defined by eqns (1) and (3a).

Thus, eqn (31a) becomes

$$\bar{A}_i\bar{X}_{i-1} + \bar{B}_i\bar{X}_i + \bar{C}_i\bar{X}_{i+1} = 0, i = 1, 2, \ldots, N-1, \tag{43}$$

where

$$\bar{A}_i = 2\bar{E}_i/\Delta\theta - \bar{F}_i, \bar{B}_i = -4\bar{E}_i/\Delta\theta + 2\bar{G}_i\Delta\theta, \bar{C}_i = 2\bar{E}_i/\Delta\theta + \bar{F}_i. \tag{44a–c}$$

The elements of the 4×4 matrices $\bar{E}_i$, $\bar{F}_i$ and $\bar{G}_i$ are given in Appendix 2.

Now, it may be shown that $u_1 = u_2 = w = w' = 0$ at $\theta = 0, \pi$ when $m \neq 1$ in order for the strains and curvatures to remain finite at the poles ($\theta = 0, \pi$). Furthermore, it is also required that $m_{11} = 0$ at $\theta = 0, \pi$ when $m \neq 0, 2$[18]. Thus, $u_1 = u_2 = w = m_{11} = 0$ at $\theta = 0, \pi$ with $m \neq 0, 1, 2$ which according to eqn (31b) gives $\bar{X} = 0$ when $\theta = 0$ and $\theta = \pi$. These boundary conditions may be written using eqn (43) with $i = 0$ for $\theta = 0$ and $i = N$ for $\theta = \pi$ as

$$\bar{B}_0\bar{X}_0 + \bar{C}_0\bar{X}_1 = 0, \text{and } \bar{A}_N\bar{X}_{N-1} + \bar{B}_N\bar{X}_N = 0, \tag{45a, b}$$

where $\bar{B}_0$ and $\bar{B}_N$ are identity matrices and $\bar{C}_0$ and $\bar{A}_N$ are null matrices.

Bifurcation occurs when the determinant of the coefficients of the $N + 1$ algebraic eqns (43) and (45) equals zero. This determinant may be expanded in the form of eqn (2) in Ref. [28] and the required eigenvalues located using the modified residual

$$\mathcal{M} = \frac{|\bar{B}_1|}{\text{abs}\,|\bar{B}_1|}\cdot\frac{|\bar{B}_2 - \bar{A}_2\bar{P}_1|}{\text{abs}\,|\bar{B}_2 - \bar{A}_2\bar{P}_1|}\cdot\frac{|\bar{B}_3 - \bar{A}_3\bar{P}_2|}{\text{abs}\,|\bar{B}_3 - \bar{A}_3\bar{P}_2|}$$
$$\frac{|\bar{B}_{N-2} - \bar{A}_{N-2}\bar{P}_{N-3}|}{\text{abs}\,|\bar{B}_{N-2} - \bar{A}_{N-2}\bar{P}_{N-3}|}\cdot|\bar{B}_{N-1} - \bar{A}_{N-1}\bar{P}_{N-2}| \tag{46}$$

where

$$\bar{P}_1 = \bar{B}_1^{-1}\bar{C}_1, \text{and } \bar{P}_i = [\bar{B}_i - \bar{A}_i\bar{P}_{i-1}]^{-1}\bar{C}_i, i = 2, \ldots, N-2. \tag{47a, b}$$

The modified residual $\mathcal{M}$ is computed at each integration time step for every circumferential harmonic (m) up to the degree n of the Legendre polynomial in the initial elastic response.

A change in sign of $\mathcal{M}$ indicates bifurcation.

DISCUSSION

The numerical results presented in Figs. 2–8, except for those marked ● in Fig. 3. were obtained for a dead-weight-type external pressure loading for which the terms related to P in eqns (11a) and (11b) were dropped. Moreover, the initial radial imperfection at $\theta = 0$, which equals ϵ according to eqn (15), is always directed radially inwards (i.e. $\bar{w} < 0$ at $\theta = 0$).

Tong and Pian[29] developed a finite-element method and examined the influence of symmetric imperfections on the static buckling behavior of an elastic spherical shell with $a/h = 82$ and $\nu = 0.3$ subjected to a dead-weight-type external pressure. The numerical results of Tong and Pian are taken from Fig. 3 of Ref. [29] and compared in Fig. 2 here with the present finite-difference calculations for the elastic case, where $p_c = 2Eh^2/[a^2\{3(1-\nu^2)\}^{1/2}]$ is the classical buckling pressure of a perfect spherical shell. It is evident that the two sets of results are virtually indistinguishable. It turns out that the behavior of the spherical shell in Fig. 2 is governed by axisymmetric buckling because bifurcation to a non-axisymmetric state never occurred at lower loads.

The axisymmetric static elastic buckling pressures in Fig. 2 were found using the method described in Ref. [24] and elsewhere. If the solution vectors $\delta\bar{Z}$ in Appendix 3† were known at every meridional station for a pressure p, then $\bar{Z} + \delta\bar{Z}$ would be obtained in the usual manner

†The governing equations for the linear elastic case have the same form as eqn (26) but with $\dot{\bar{Z}}^*$ and $\dot{\bar{Z}}$ replaced by $\delta\bar{Z}^*$ and δZ, respectively. A few elements in the matrix A and all those in the vector $\bar{P}$ are changed as shown in Appendix 3.

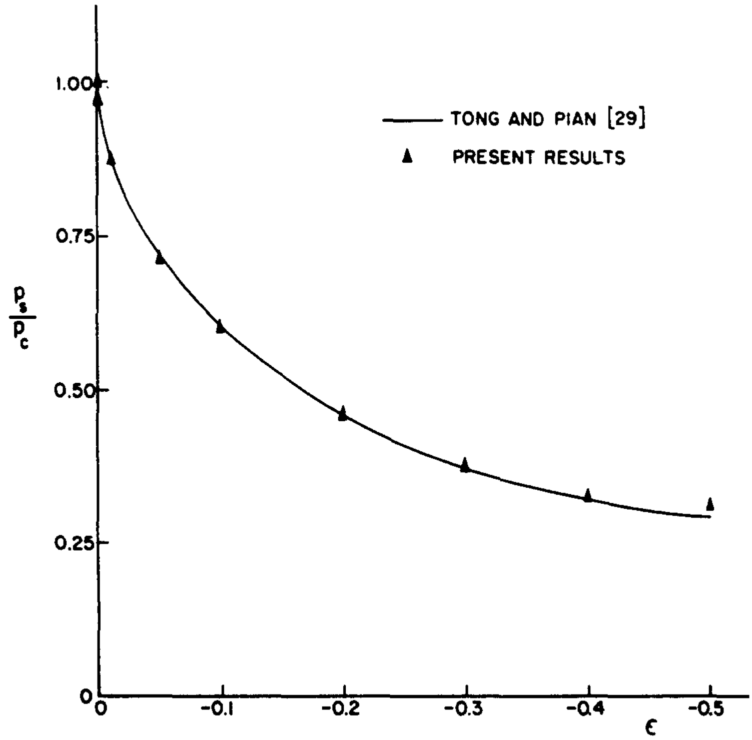

Fig. 2. Comparison of present theoretical predictions for static elastic buckling of externally pressurised complete spherical shells with the finite-element results of Tong and Pian[29] ($\mu = 1/82$, $\nu = 0.3$, $n = 16$).

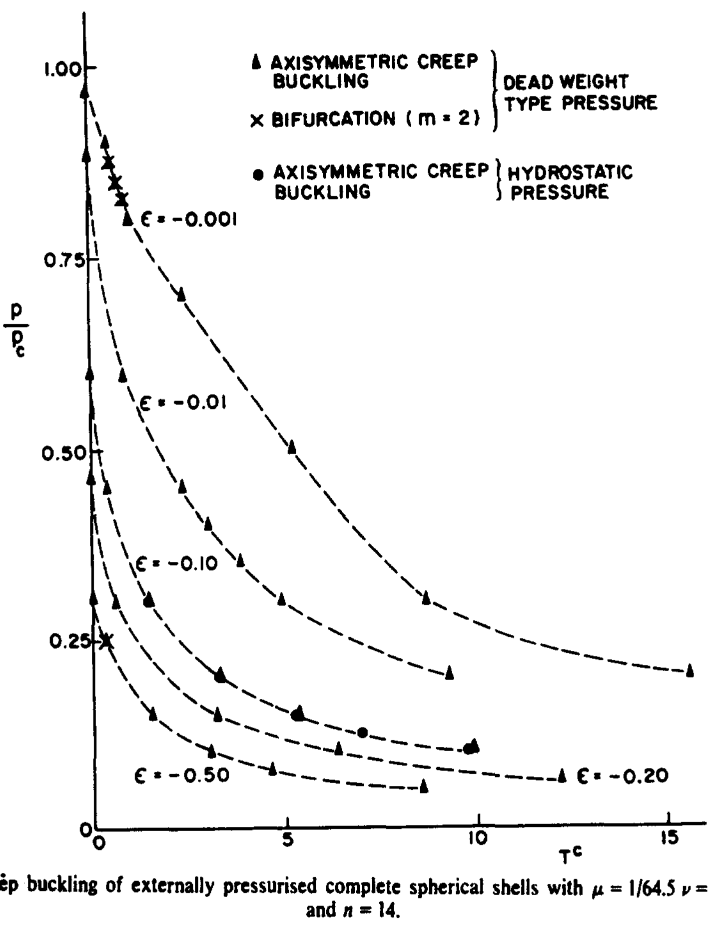

Fig. 3. Creep buckling of externally pressurised complete spherical shells with $\mu = 1/64.5$ $\nu = 1/3$. $N = 3$ and $n = 14$.

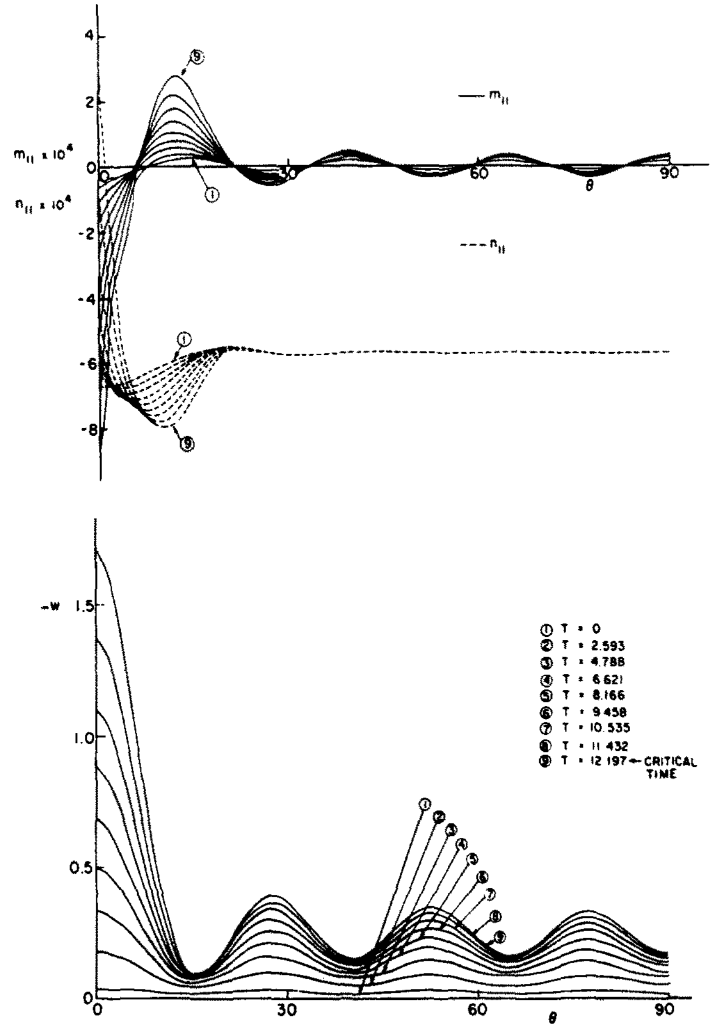

Fig. 4. Spatial and temporal variation of w, m_{11} and n_{11} for a spherical shell with $\mu = 1/64.5$, $\nu = 1/3$, $N = 3$, $n = 14$, $\epsilon = -0.2$ and $p/p_c = 0.06$.

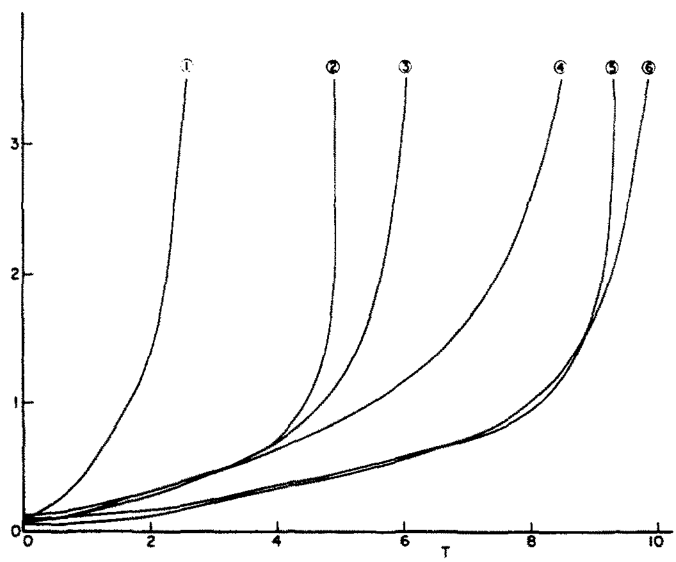

Fig. 5. Growth of radial displacement at pole ($\theta = 0$) for a spherical shell with $\mu = 1/64.5$, $\nu = 1/3$, $N = 3$ and $n = 14$ and where ①: $p/p_c = 0.10$, $\epsilon = -0.5$, $T^c = 3.0702$, ②: $p/p_c = 0.3$, $\epsilon = -0.01$, $T^c = 4.95135$, ③: $p/p_c = 0.1$, $\epsilon = -0.2$, $T^c = 6.38615$, ④: $p/p_c = 0.05$, $\epsilon = -0.5$, $T^c = 8.63307$, ⑤: $p/p_c = 0.2$, $\epsilon = -0.01$, $T^c = 9.32410$, ⑥: $p/p_c = 0.1$, $\epsilon = -0.1$, $T^c = 9.91795$.

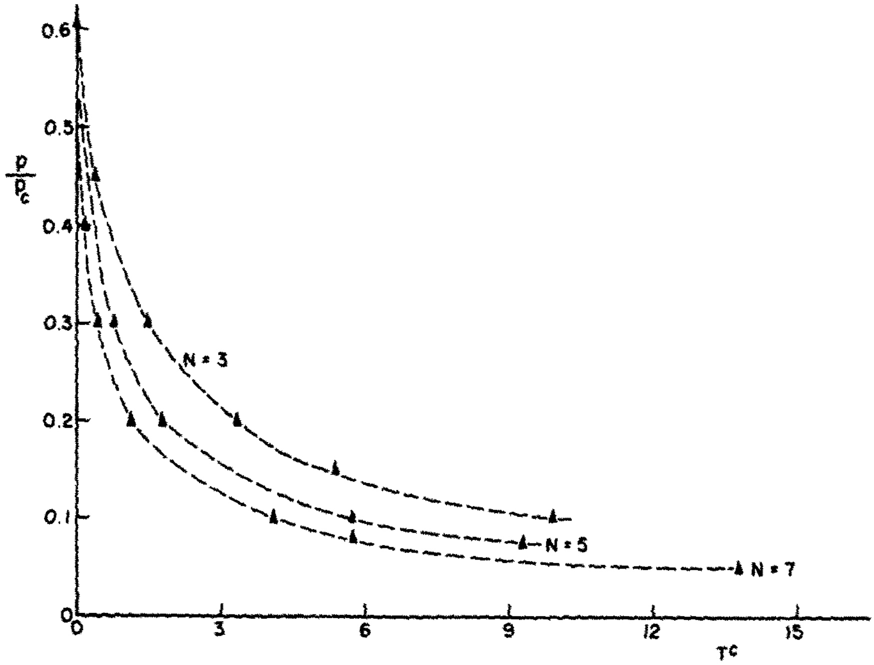

Fig. 6. Influence of creep index N on the creep buckling of complete spherical shells with $\epsilon = -0.1$, $\mu = 1/64.5$, $\nu = 1/3$ and $n = 14$.

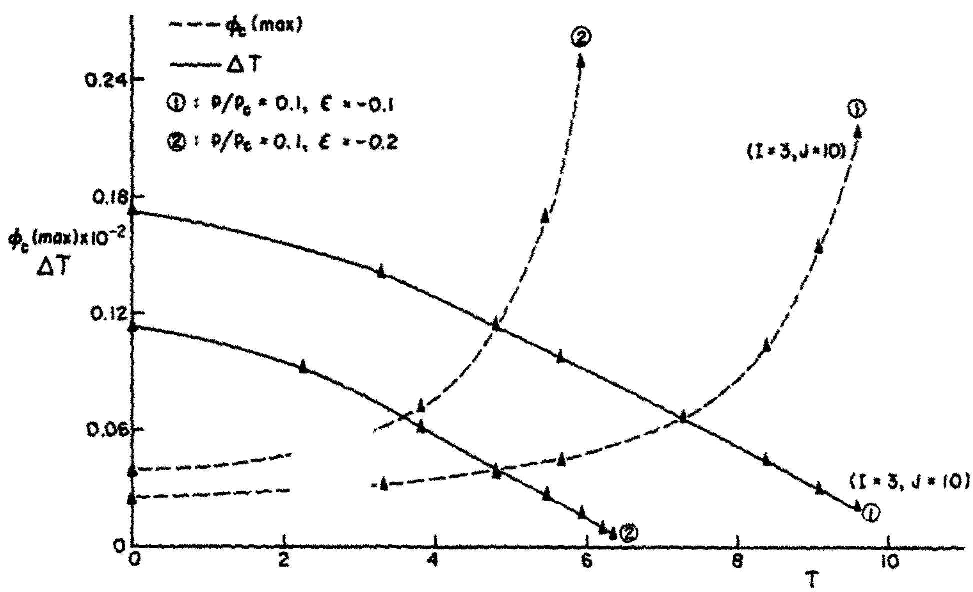

Fig. 7. Variation of ϕ_c(max) and ΔT with T for a complete spherical shell with $\mu = 1/64.5$, $\nu = 1/3$, $N = 3$, $n = 14$, and $f = 0.5$. ϕ_c(max) occurs at the location $I = 1$, $J = 1$ unless otherwise specified, where I is the station in the meridional sense with $I = 1$ at the pole, and J is the integration point across the shell thickness.

for the pressure $p + \delta p$. Convergence is assumed when

$$\left[\left\{\sum^{N} (\delta\bar{Z})^2\right\}\Big/\left\{\sum^{N} (\bar{Z})^2\right\}\right]^{1/2}$$

is less than 10^{-3}. If the convergence criterion is not satisfied after 20 iterations then the pressure is reduced by $\delta p/5$ and the process repeated. This procedure is repeated until a pressure is found at which convergence is achieved.

The dead-weight-type external pressure to classical buckling pressure ratio (p/p_c) vs the dimensionless critical time at which creep buckling occurs (T^c) is shown in Fig. 3 for a

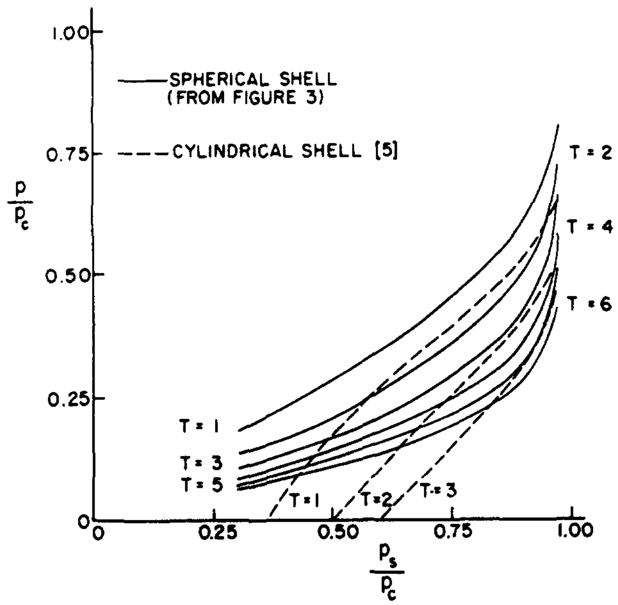

Fig. 8. Comparison of results from Fig. 3 for an externally pressurised spherical shell with those for an "equivalent" axially loaded cylindrical shell from Obrecht[5].

complete spherical shell with various magnitudes of initial imperfections. It is evident that axisymmetric creep buckling essentially governs the response since bifurcation into a non-axisymmetric state only occurs for a few shells with short creep buckling times and at pressures which are quite close to the axisymmetric creep buckling results. The meridional distribution and temporal variation of the non-dimensional radial displacement (w), dimensionless meridional bending moment (m_{11}), and dimensionless meridional membrane force (n_{11}) are indicated in Fig. 4, while the typical dimensionless radial displacement-time histories in Fig. 5 reveal the growth of the inwards displacements at the pole for several of the data points in Fig. 3. The numerical results in Fig. 6 serve to demonstrate the influence of the creep index N on the creep buckling pressure-critical time characteristics.

The non-dimensionalised time step given by eqn (42) ensures numerical stability of the time integration scheme for the axisymmetric creep buckling calculations. A value of $f = 0.5$ was used for all the results presented herein. Furthermore, the factor $4f(1+\nu)/3N$ equals 0.296, 0.178 and 0.127 for $N = 3$, 5 and 7 respectively and $\nu = 1/3$. Thus, the two different numerical stability criteria developed in Refs. [26, 27] are satisfied. Now, eqn (42) may be written in the form

$$\Delta T = 2f(1+\nu)/\{N\phi_c(\max)\},$$

where $\phi_c(\max)$ is defined by eqn (14a) with $\mathcal{J}_2$ replaced by $\mathcal{J}_2(\max)$. The growth of the factor $\phi_c(\max)$ is constructed in Fig. 7 for two particular cases using the largest values of $\mathcal{J}_2$ which most often occurred at the integration point[25] nearest the outer surface of the spherical shell at a pole. The associated temporal variation of the dimensionless time steps (ΔT) according to eqn (42) are also shown in Fig. 7. It was assumed that axisymmetric creep buckling occurred when the criterion $\Delta T/T < \xi$ with $\xi = 10^{-3}$ was satisfied.

It should be noted that for small enough ξ then axisymmetric creep buckling could occur prior to bifurcation for the four cases $p/p_c = 0.825$, 0.850 and 0.875 with $\epsilon = -0.001$ and $p/p_c = 0.25$ with $\epsilon = -0.5$ in Fig. 3. Bifurcation into a non-axisymmetric state occurred when the respective non-dimensional radial displacements at the poles ($w(0)$) of the two cases $p/p_c = 0.825$ and 0.875 equalled -0.07244 and -0.92249 with associated dimensionless creep buckling times T^c of 0.87640, and 0.58761. Axisymmetric creep buckling with $\xi = 10^{-3}$ developed for these two cases when $w(0)$ was -3.16320 and -3.51870 with T^c equal to 0.91561 and 0.60168, respectively.

Some numerical creep buckling calculations for the hydrostatic pressure loading case, which requires the retention of the terms related to P in eqns (11a) and (11b) are presented in Fig. 3. It is evident from these results that there is no practical difference between the creep buckling behavior of complete spherical shells subjected to hydrostatic or dead-weight-type pressures, at least for the parameters examined.

The numerical creep buckling results presented in the previous figures are replotted in Fig. 8 with the non-dimensional external pressure ratio (p/p_c) as the ordinate and a measure of the imperfection (p_s/p_c) as the abscissa. Also indicated in Fig. 8 are some numerical results for the creep buckling of axially loaded cylindrical shells which were taken from Fig. 2 in Ref. [5]. This comparison is made for axially loaded cylindrical shells and externally pressurised spherical shells with the same a/h ratios and material properties and having the same effective stresses. It is evident that the critical times for the creep buckling of spherical shells are longer than those for "equivalent" cylindrical shells. A similar situation was also found in Ref. [13] wherein it was shown that the radial displacements of externally pressurised cylindrical shells grew much more rapidly than those for externally pressurised spherical shells. In passing, it should be noted that Obrecht's results in Fig. 2 of Ref. [5], some of which are reproduced in Fig. 8 here, predict finite creep buckling times when $p/p_c = 0$ which does not appear acceptable from a physical viewpoint.

A direct quantitative comparison cannot be made between the experimental results on externally pressurised hemispherical shells reported in Ref. [30] and the predictions of the numerical procedure presented herein because the initial imperfections of the experimental models were not recorded. Moreover, the creep characteristics of lead were not measured in Ref. [30] which as remarked in Ref. [31] should be obtained for the same batch of material as used in the experimental tests. In any event, the following qualitative comparisons may be of some value.

Tong and Greenstreet [30] found that the creep buckling of hemispherical shells was very sensitive to the presence of geometrical imperfections. The numerical results for the complete spherical shells in Figs. 3 and 8 here also reveal a strong sensitivity to the magnitude of the initial geometric imperfections. Furthermore, Tong and Greenstreet observed that the collapse of the shells was usually very violent which is in accord with the rapid growth of the radial displacements near the critical time indicated in Fig. 5. It appears that the buckled shells in Ref. [30] had various deformed shapes some of which were nearly axisymmetric, while others were non-symmetric. Tong and Greenstreet uncovered no obvious correlation between the deformed shapes of the buckled shells and life and in this regard it is interesting to observe from Fig. 3 that the axisymmetric creep buckling and bifurcation pressures for spherical shells with radially inwards initial imperfections were quite close within certain ranges of the parameters.

Experimental investigations into the creep buckling behavior of boss loaded hemispherical shells and externally pressurised shallow shells are reported in Ref. [32, 33], respectively. These particular cases have not been examined herein but the temporal characteristics of the radial displacements are similar to those in Fig. 5 in that they grow very rapidly near the critical times.

The influences of primary creep, post-buckling behavior, and material plasticity have not been included in the numerical method developed in this article. Murakami and Tanaka [3] have shown that primary creep can exercise an important effect on the creep buckling behavior of cylindrical shells. The post-buckling characterics are probably not very important from a practical viewpoint for the problem examined herein because bifurcation controls the behavior only within the restricted range of parameters indicated in Fig. 3 for which the associated pressures are only slightly different from the corresponding axisymmetric creep buckling values. The authors intend to examine the influence of material plasticity by retaining in eqn (4) the appropriate expressions for plastic strain increments [17] since it might be quite important for spherical shells without large yield stresses or having relatively small a/h ratios.

CONCLUSIONS

The numerical finite-difference results for the elastic buckling of externally pressurised imperfect spherical shells agree very closely with the numerical finite-element results of Tong and Pian [29] as shown in Fig. 2.

The numerical results in the various figures indicate that initial imperfections exercise an important influence on the critical times for the creep buckling of complete spherical shells subjected to external pressures. It appears from the numerical calculations that the creep buckling behavior of a complete spherical shell is very similar for hydrostatic and dead-weight-type external pressures, at least for the particular parameters examined herein. It turns out from a practical viewpoint that axisymmetric creep buckling governs the behavior of the spherical shells investigated in this article with initial imperfections described by eqn (15) but acting radially inwards at the pole.

It was observed from the present results that the creep buckling times of externally pressurised complete spherical shells are longer than those for "equivalent" axially loaded cylindrical shells.

Acknowledgements—The authors are indebted to the Solid Mechanics Program of the National Science Foundation for their support of the work reported herein under contract number ENG 75-13642 with the Massachusetts Institute of Technology. The authors also wish to take this opportunity to express their appreciation to Prof. T. H. H. Pian of M.I.T.

REFERENCES

1. N. J. Hoff, Creep buckling of plates and shells. *Proc. 13th Int. Cong. Theoretical and Appl.Mech.* (Edited by E. Becker and G. K. Mikhailov), pp. 124–140. Springer-Verlag, Berlin (1973).
2. J. C. Gerdeen and V. K. Sazawal, *A Review of Creep Instability in High Temperature Piping and Pressure Vessels, Welding Research Council Bulletin* No. 195, 33–56 (1974).
3. S. Murakami and E. Tanaka, On the creep buckling of circular cylindrical shells. *Int. J. Mech. Sci.* **18**, 185–194 (1976).
4. N. Jones and P. F. Sullivan, On the creep buckling of a long cylindrical shell. *Int. J. Mech. Sci.* **18**, 209–213 (1976).
5. H. Obrecht, Creep buckling and postbuckling of circular cylindrical shells under axial compression. *Int. J. Solids Structures* **13**, 337–355 (1977).
6. N. C. Huang, Axisymmetrical creep buckling of clamped shallow shells. *J. Appl. Mech.* **32**, 323–330 (1965).
7. P. Varpasuo, Asymmetric form of stability loss of a shallow spherical shell with limited creep of the material. *Sov. Appl. Mech.* **10**, 940–945 (1976).
8. N. Miyazaki, G. Yagawa and Y. Ando, A parametric analysis of creep buckling of shallow spherical shell by the finite element method, contributed at the *Joint Petroleum Mech. Eng. and Pressure Vessels and Piping Conf.* Mexico (Sept. 1976).
9. N. C. Huang and G. Funk, Inelastic buckling of a deep spherical shell subject to external pressure. *AIAA J.* **12**, 914–920 (1974).
10. S. Takezono and K. Inoue, Elastic-plastic creep deformations of axisymmetrical shells. *Bulletin of JSME* **19**, 226–232 (1976).
11. J. W. Hutchinson, On the postbuckling behavior of imperfection-sensitive structures in the plastic range. *J. Appl. Mech.* **39**, 155–162 (1972).
12. J. W. Hutchinson and W. T. Koiter, Postbuckling theory. *Appl. Mech. Rev.* **23**, 1353–1366 (1970).
13. N. Jones, Creep buckling of a complete spherical shell. *J. Appl. Mech.* **43**, 450–454 (1976).
14. D. Bushnell, Bifurcation buckling of shells of revolution including large deflections, plasticity and creep. *Int. J. Solids Structures* **10**, 1287–1305 (1974); *Stress, buckling and vibration of hybrid bodies of revolution, presented at AIAA/ASME/SAE 17th structures, structural dynamics and materials conference* (May 1976).
15. J. L. Sanders, Nonlinear theories for thin shells. *Quart. Appl. Math.* **21**, 21–36 (1963).
16. W. T. Koiter, The non-linear buckling problem of a complete spherical shell under uniform external pressure. *Proc. Kon. Ned. Akad. Wetenschappen* **72B**, 40–123 (1969).
17. N. Jones and C. S. Ahn, Dynamic elastic and plastic buckling of complete spherical shells. *Int. J. Solids Structures* **10**, 1357–1374 (1974).
18. P. C. Xirouchakis and N. Jones, *Axisymmetric and Bifurcation Creep Buckling of Externally Pressurised Spherical Shells, M.I.T., Department of Ocean Engineering Report* 78-6, (Oct. 1978).
19. A. Kalnins, Analysis of shells of revolution subject to symmetrical and nonsymmetrical loads. *J. Appl. Mech.* **33**, 467–476 (1964).
20. W. B. Stephens and R. E. Fulton, Axisymmetric Static and Dynamic Buckling of Spherical Caps Due to Centrally Distributed Pressures. *AIAA J.* **7**, 2120–2126 (1969).
21. G. A. Greenbaum and D. C. Conroy, Postwrinkling behavior of a conical shell of revolution subject to bending loads. *AIAA J.* **8**, 700–707 (1970).
22. E. I. Grigoliuk and Y. V. Lipovtsev, On the creep buckling of shells. *Int. J. Solids Structures* **5**, 155–173 (1969).
23. M. L. Potters, *A Matrix Method For the Solution of a Linear Second Order Difference Equation in Two Variables, Report MR*19. Mathematisch Centrum, Amsterdam (1955).
24. W. B. Stephens, Computer program for static and dynamic axisymmetric nonlinear response of symmetrically loaded orthotropic shells of revolution. *NASA Tech. Note* TN D-6158 (Dec. 1970).
25. B. Carnahan, H. A. Luther and J. O. Wilkes, Applied Numerical Methods. Wiley, New York (1969).
26. I. Cormeau Numerical stability in quasi-static elasto/visco-plasticity. *Int. J. Num. Meth. Engng* **9**, 109–127 (1975).
27. T. Shimizu, Axisymmetric creep analysis by assumed stress hybrid finite-element method, M. S. Thesis. Dept. of Aeronautics and Astronautics, M.I.T. (1974).
28. R. E. Blum and R. E. Fulton, A modification of Potters' method for solving eigenvalue problems involving tridiagonal matrices. *AIAA J.* **4**, 2231–2232 (1966).
29. P. Tong and T. H. H. Pian, Postbuckling analysis of shells of revolution by the finite-element method, *Thin-Shell Structures: Theory, Experiment, and Design* (Edited by Y. C. Fung and E. E. Sechler), pp. 435–452, Prentice-Hall, New Jersey (1974).

30. K. N. Tong and B. L. Greenstreet, Experimental observations on creep buckling of spherical shells, collected papers on instability of shell structures, *NASA Tech. Note* D-1510, 587–596 (1962).
31. P. T. Tarpgaard and N. Jones, The influence of finite-deformations upon the creep behavior of circular plates, *Int. J. Mech. Sci.* **14**, 447–467 (1972).
32. R. K. Penny and D. L. Marriott, *Design for Creep*. McGraw-Hill, New York (1971).
33. J. J. J. Shi, C. D. Johnson and N. R. Bauld, Application of the variational theorem for creep of shallow spherical shells, *AIAA J.* **8**, 469–476 (1970).

APPENDIX 1

The elements of the matrix $\bar{A}$ and vector $\bar{P}$ en eqn (26) are

$$A_{11} = (1-\nu)\cot\theta - (\phi + \bar{\phi}),\ A_{12} = 1,\ A_{13} = 0,\ A_{14} = -\mu\cot^2\theta,$$
$$A_{15} = -\mu\cot\theta,\ A_{16} = -(n_{11} + P),\ A_{21} = -\{1 + \nu + (\phi + \bar{\phi})^* + \nu(\phi + \bar{\phi})\cot\theta$$
$$+ (\phi + \bar{\phi})^2\},\ A_{22} = \cot\theta + \phi + \bar{\phi},\ A_{23} = -12(1-\nu^2)n_{11}/\mu,$$
$$A_{24} = -\mu\cot\theta\{1 + \cot\theta(\phi + \bar{\phi})\},\ A_{25} = -\mu\{1 + \cot\theta(\phi + \bar{\phi})\},$$
$$A_{26} = -n^{\dagger}_{1} - n_{11}\cot\theta + \nu\cot\theta n_{11} - (\phi + \bar{\phi})(n_{11} + P),\ A_{31} = 0,$$
$$A_{32} = -1/\mu,\ A_{33} = (1-\nu)\cot\theta,\ A_{34} = A_{35} = 0,$$
$$A_{36} = -\mu\cot^2\theta/12,\ A_{41} = -(1-\nu^2)/\mu,\ A_{42} = A_{43} = 0,$$
$$A_{44} = \nu\cot\theta,\ A_{45} = 1 + \nu,\ A_{46} = (\phi + \bar{\phi})/\mu,\ A_{51} = A_{52} = A_{53} = 0,$$
$$A_{54} = -1,\ A_{55} = 0,\ A_{56} = 1/\mu,\ A_{61} = A_{62} = 0,$$
$$A_{63} = -12(1-\nu^2)/\mu,\ A_{64} = A_{65} = 0,\ A_{66} = \nu\cot\theta,$$
$$P_1 = \cot\theta\int_{-1/2}^{1/2}\phi_c(\sigma_{11} - 2\sigma_{22})\,d\zeta/3,$$
$$P_2 = \{1 + \cot\theta(\phi + \bar{\phi})\}\int_{-1/2}^{1/2}\phi_c(\sigma_{11} - 2\sigma_{22})\,d\zeta/3 + 4n_{11}\int_{-1/2}^{1/2}\phi_c\{(2-\nu)\sigma_{11} - (1-2\nu)\sigma_{22}\}\zeta\,d\zeta/\mu,$$
$$P_3 = \cot\theta\int_{-1/2}^{1/2}\phi_c(\sigma_{11} - 2\sigma_{22})\zeta\,d\zeta/3,$$
$$P_4 = \int_{-1/2}^{1/2}\phi_c\{(2-\nu)\sigma_{11} - (1-2\nu)\sigma_{22}\}\,d\zeta/3\mu,$$
$$P_5 = 0$$
$$P_6 = 4\int_{-1/2}^{1/2}\phi_c\{(2-\nu)\sigma_{11} - (1-2\nu)\sigma_{22}\}\zeta\,d\zeta/\mu.$$

APPEXDIX 2

The elements of the matrices $\bar{E}$, $\bar{F}$ and $\bar{G}$ in eqn (31a) are

$$E_{11} = \mu/(1-\nu^2),\ E_{12} = 0,\ E_{13} = -\mu(\bar{\phi}_1 + \dot{\bar{\phi}}_1)/(1-\nu^2),\ E_{14} = 0,$$
$$E_{21} = 0,\ E_{22} = \mu\sin\theta(1 + \mu^2/12)/\{2(1+\nu)\} + \mu(\bar{n}_{11} + \bar{n}_{22})\sin\theta/4,$$
$$E_{23} = -m\mu^3/\{12(1+\nu)\},\ E_{24} = 0,\ E_{31} = E_{13},\ E_{32} = E_{23}\operatorname{cosec}\theta,$$
$$E_{33} = \mu^3\{(1+\nu)\cot^2\theta + 2m^2\operatorname{cosec}^2\theta\}/\{12(1+\nu)\} + \mu(\bar{\phi}_1 + \dot{\bar{\phi}}_1)^2/(1-\nu^2)$$
$$+ \mu\bar{n}_{11},\ E_{34} = \mu,\ E_{41} = E_{42} = 0,\ E_{43} = -\nu,\ E_{44} = 0.$$

$$F_{11} = \mu\cot\theta/(1-\nu^2),\ F_{12} = -m\mu\operatorname{cosec}\theta[1/(1-\nu) + \mu^2/\{12(1+\nu)\}]/2 + \mu m(\bar{n}_{11} + \bar{n}_{22})\operatorname{cosec}\theta/4,$$
$$F_{13} = \mu[-(\bar{\phi}_1 + \dot{\bar{\phi}}_1)^* + (\bar{\phi}_1 + \dot{\bar{\phi}}_1)\{(\bar{\phi}_1 + \dot{\bar{\phi}}_1) - (1-\nu)\cot\theta\} + 1 + \nu]/(1-\nu^2)$$
$$+ \mu\bar{n}_{11} + \mu^3\{(1+\nu)\cot^2\theta + m^2\operatorname{cosec}^2\theta\}/\{12(1-\nu)\} + \mu P,$$
$$F_{14} = \mu,\ F_{21} = -F_{12}\sin\theta,\ F_{22} = E_{22}\cot\theta + \mu(\bar{n}^{\dagger}_{1} + \bar{n}^{\dagger}_{2})\sin\theta/4,$$
$$F_{23} = -m\mu[(\bar{\phi}_1 + \dot{\bar{\phi}}_1)/\{2(1-\nu)\} + \mu^2\cot\theta/12],\ F_{24} = 0,$$
$$F_{31} = -\mu^3\{\cot^2\theta + m^2\operatorname{cosec}^2\theta/(1+\nu)\}/12 - \mu[1 + \nu + (\bar{\phi}_1 + \dot{\bar{\phi}}_1)^*$$
$$+ (\bar{\phi}_1 + \dot{\bar{\phi}}_1)\{\bar{\phi}_1 + \dot{\bar{\phi}}_1 + (1+\nu)\cot\theta\}]/(1-\nu^2) - \mu\bar{n}_{11},\ F_{32} = -F_{23}\operatorname{cosec}\theta,$$
$$F_{33} = -\mu^3\{1 + \nu + (1 + \nu + 2m^2)\operatorname{cosec}^2\theta\}\cot\theta/\{12(1+v)\}$$
$$+ \mu(\bar{\phi}_1 + \dot{\bar{\phi}}_1)\{2(\bar{\phi}_1 + \dot{\bar{\phi}}_1)^* + (\bar{\phi}_1 + \dot{\bar{\phi}}_1)\cot\theta\}/(1-\nu^2) + \mu(\bar{n}^{\dagger}_{1} + \bar{n}_{11}\cot\theta),$$
$$F_{34} = (2-\nu)\mu\cot\theta,\ F_{41} = \nu,\ F_{42} = 0,\ F_{43} = -\nu^2\cot\theta,\ F_{44} = 0.$$
$$G_{11} = \mu[(\bar{\phi}_1 + \dot{\bar{\phi}}_1)^* + (\bar{\phi}_1 + \dot{\bar{\phi}}_1)\{(1-2\nu)\cot\theta - (\bar{\phi}_1 + \dot{\bar{\phi}}_1)\} - \nu$$
$$- \cot^2\theta - (1-\nu)m^2\operatorname{cosec}^2\theta/2]/(1-\nu^2) - \mu^3\{(1+\nu)\cot^2\theta$$
$$+ m^2\operatorname{cosec}^2\theta/2\}/\{12(1+\nu)\} - \mu\bar{n}_{11} - \mu m^2(\bar{n}_{11} + \bar{n}_{22})\operatorname{cosec}^2\theta/4 - \mu P,$$

$$G_{12}=m\mu\ \mathrm{cosec}\ \theta[\{\bar{3}\nu-1\}(\bar{\phi}_1+\tilde{\phi}_1)+(3-\nu)\cot\theta\}/(1-\nu)$$
$$+\mu^2(3+2\nu)\cot\theta/12]/\{2(1+\nu)\}+\mu m(\bar{n}_{11}+\bar{n}_{22})\cot\theta\ \mathrm{cosec}\ \theta/4,$$
$$G_{13}=\mu(\bar{\phi}_1+\tilde{\phi}_1)[m^2\ \mathrm{cosec}^2\ \theta/\{2(1+\nu)\}-1/(1-\nu)]$$
$$-\mu^3m^2(2+\nu)\cot\theta\ \mathrm{cosec}^2\ \theta/\{12(1+\nu)\},\ G_{14}=\mu(1-\nu)\cot\theta,$$
$$G_{21}=G_{12}\sin\theta-\mu m(\bar{n}^*_{11}+\bar{n}^*_{22})/4,\ G_{22}=\mu[-m^2\ \mathrm{cosec}\ \theta+(1-\nu)\{(2\cos\theta$$
$$-(\bar{\phi}_1+\tilde{\phi}_1)\sin\theta)(\bar{\phi}_1+\tilde{\phi}_1-\cot\theta)+(\bar{\phi}_1+\tilde{\phi}_1)^*\sin\theta+\mathrm{cosec}\ \theta\}/2]/(1-\nu^2)$$
$$+\mu^3\sin\theta[-\cot^2\theta+\{1/2-m^2(1+\nu)\}\mathrm{cosec}^2\ \theta]/12(1+\nu)\}$$
$$-\mu\bar{n}_{22}\sin\theta+\mu\{-(\bar{n}_{11}+\bar{n}_{22})\mathrm{cosec}\ \theta+(\bar{n}^*_{11}+\bar{n}^*_{22})\cos\theta\}/4-\mu P\sin\theta,$$
$$G_{23}=m\mu[1/(1-\nu)-\{(\bar{\phi}_1+\tilde{\phi}_1)(2\cot\theta-\bar{\phi}_1-\tilde{\phi}_1)+(\bar{\phi}_1+\tilde{\phi}_1)^*$$
$$-(\bar{\phi}_1+\tilde{\phi}_1)\cot\theta\}/\{2(1+\nu)\}]+m\mu^3[\cot^2\theta+\{m^2(1+\nu)$$
$$-1\}\mathrm{cosec}^2\ \theta]/\{12(1+\nu)\}+\mu m\bar{n}_{22}+m\mu P,\ G_{24}=\mu\nu m,$$
$$G_{31}=\mu^3\{1+(1-m^2)\mathrm{cosec}^2\ \theta\}\cot\theta/12-\mu[(1+\nu)\{\cot\theta$$
$$+(\bar{\phi}_1+\tilde{\phi}_1)\}+\{(\bar{\phi}_1+\tilde{\phi}_1)^*+(\bar{\phi}_1+\tilde{\phi}_1)\cot\theta\}(\bar{\phi}_1+\tilde{\phi}_1+\nu\cot\theta)$$
$$+(\bar{\phi}_1+\tilde{\phi}_1)\{(\bar{\phi}_1+\tilde{\phi}_1)^*-\nu\ \mathrm{cosec}^2\ \theta\}$$
$$-(1-\nu)m^2(\bar{\phi}_1+\tilde{\phi}_1)\mathrm{cosec}^2\ \theta/2]/(1-\nu^2)-\mu(\bar{n}^*_{11}+\bar{n}_{11}\cot\theta),$$
$$G_{32}=-\mu^3m\ \mathrm{cosec}\ \theta\{2+\nu+(1+\nu)(\cot^2\theta-m^2\ \mathrm{cosec}^2\ \theta)\}/\{12(1+\nu)\}$$
$$+\mu m\ \mathrm{cosec}\ \theta\{1+\nu+\nu(\bar{\phi}_1+\tilde{\phi}_1)^*$$
$$+(1-\nu)(\bar{\phi}_1+\tilde{\phi}_1)(\bar{\phi}_1+\tilde{\phi}_1-\cot\theta)/2\}/(1-\nu^2)+\mu m\ \mathrm{cosec}\ \theta\bar{n}_{22},$$
$$G_{33}=\mu^3m^2\ \mathrm{cosec}^2\ \theta\{2\ \mathrm{cosec}^2\ \theta+(1+\nu)(1+2\cot^2\theta-m^2\ \mathrm{cosec}^2\ \theta)\}/\{12(1+\nu)\}$$
$$-\mu m^2\ \mathrm{cosec}^2\ \theta\bar{n}_{22}+\mu[-\{2+(\bar{\phi}_1+\tilde{\phi}_1)^*$$
$$+(\bar{\phi}_1+\tilde{\phi}_1)\cot\theta\}/(1-\nu)-m^2(\bar{\phi}_1+\tilde{\phi}_1)^2\mathrm{cosec}^2\ \theta/\{2(1+\nu)\}],$$
$$G_{34}=-\mu(1-\nu+\nu m^2\ \mathrm{cosec}^2\ \theta),\ G_{41}=\nu^2\cot\theta,$$
$$G_{42}=-\nu^2m\ \mathrm{cosec}\ \theta,\ G_{43}=\nu^2m^2\ \mathrm{cosec}^2\ \theta,\ G_{44}=-12\nu(1-\nu^2)/\mu^2.$$

APPENDIX 3

The rate formulation which was used to derive eqn (26) is not suitable for the static axisymmetric elastic buckling case. Thus, it is assumed that $n_{11}^{(p+\delta p)}=n_{11}^{(p)}+\delta n_{11}$, where $n_{11}^{(p)}$ is the value at the pressure p, while δn_{11} is the incremental change in n_{11} when the pressure is increased by an incremental amount to $p+\delta p$. Similarly, $q^{(p+\delta p)}=q^{(p)}+\delta q$, $m_{11}^{(p+\delta p)}=m_{11}^{(p)}+\delta m_{11}$, $u^{(p+\delta p)}=u^{(p)}+\delta u$, $w^{(p+\delta p)}=w^{(p)}+\delta w$, and $\phi^{(p+\delta p)}=\phi^{(p)}+\delta\phi$. In this circumstance, eqn (26) for dead-weight type pressure loading is replaced by $\delta\bar{Z}^*+\bar{A}\delta\bar{Z}=\bar{P}$, where $\delta\bar{Z}=[\delta n_{11},\delta q,\delta m_{11},\delta u,\delta w,\delta\phi]^T$, $\bar{A}$ is given in Appendix 1 except

$$A_{16}=-n_{11},\ A_{21}=-\{1+\nu+\tilde{\phi}^*+\nu\tilde{\phi}\cot\theta+(\phi+\tilde{\phi})^2+12(1-\nu^2)m_{11}/\mu\},$$
$$A_{26}=-\{2(\phi+\tilde{\phi})n_{11}-q+\mu u\cot^2\theta+\mu w\cot\theta\},$$

and

$$P_1=-n^*_{11}-\{(1-\nu)\cot\theta-(\phi+\tilde{\phi})\}n_{11}-q+\mu u\cot^2\theta+\mu w\cot\theta,$$
$$P_2=P-q^*+\{1+\nu+\tilde{\phi}^*+\nu\tilde{\phi}\cot\theta+(\phi+\tilde{\phi})^2\}n_{11}$$
$$-(\cot\theta+\phi+\tilde{\phi})q+12(1-\nu^2)n_{11}m_{11}/\mu+\mu\{1+(\phi+\tilde{\phi})\cot\theta\}u\cot\theta+\mu\{1+(\phi+\tilde{\phi})\cot\theta\}w,$$
$$P_3=-m^*_{11}+q/\mu-(1-\nu)m_{11}\cot\theta+\mu\phi\cot^2\theta/12,$$
$$P_4=-u^*+(1-\nu^2)n_{11}/\mu-\nu u\cot\theta-(1+\nu)w-(\phi/2+\tilde{\phi})\phi/\mu,$$
$$P_5=-w^*+u-\phi/\mu,$$
$$P_6=-\phi^*+12(1-\nu^2)m_{11}/\mu-\nu\phi\cot\phi,$$

where the superscripts p have been omitted for convenience.